

Correlative Analysis of Nanoparticles

In recent years, nanoparticles have emerged as a platform for bioscience, nanoengineering, and chemistry [1], [2]. Due to their unique scale (1-500 nm) at the boundary between atomic (0.6 nm) and bulk materials, nanoparticles feature unique properties. Nanoparticles' incredibly small-scale results in a massive surface area to volume ratio and allows them to exhibit quantum effects, a famous example of such being quantum dots [3], [4]. In many applied and analytical contexts, nanoparticles larger than ~10 nm are of particular interest, as they exhibit stable ensemble behavior while remaining challenging to characterize due to their dimensions being below the wavelength of visible light. While large groups of nanoparticles can still be resolved optically, studying small clusters or even individual nanoparticles typically requires an SEM.

Defined by size rather than composition, nanoparticles can be fabricated from a wide range of materials with distinct properties. Metal oxides are used in biological imaging, semiconductors in nanophotonics, and ceramics in drug delivery applications [5], [6], [7]. In addition, surface coatings — such as polyethylene glycol — are commonly applied to modify nanoparticle behavior, for example by reducing immune recognition in drug delivery systems [8].

The FusionScope provides a powerful platform for nanoparticle analysis, addressing the limitations of optical microscopy and the need for precise size, topography, and compositional measurements. Its integrated SEM enables localization of individual nanoparticles, AFM provides high-precision size and surface characterization, and EDS delivers elemental information to distinguish nanoparticle coatings.

In this study, the FusionScope was used to analyze a mixed sample of iron oxide nanoparticles, including uncoated, carboxyl-functionalized particles [9], and gold-coated particles sourced from nanoComposix [10]. The differing surface chemistries enable distinct functionalization strategies for medical applications. Nanoparticles were deposited onto a TEM grid, whose thin carbon support minimizes background signal and distortion in EDS measurements.

Measurement

SEM

Due to the diffraction limit of conventional optics, optical microscopes provide only coarse localization of sub-micron nanoparticles and cannot reliably distinguish large particles from closely spaced clusters. As shown in [Figure 1 \(A\)](#), clusters of small nanoparticles appear indistinguishable from single larger particles, whereas the SEM image of the same region ([Figure 1 \(B\)](#)) clearly resolves individual nanoparticles, enabling accurate analysis of clustering behavior.

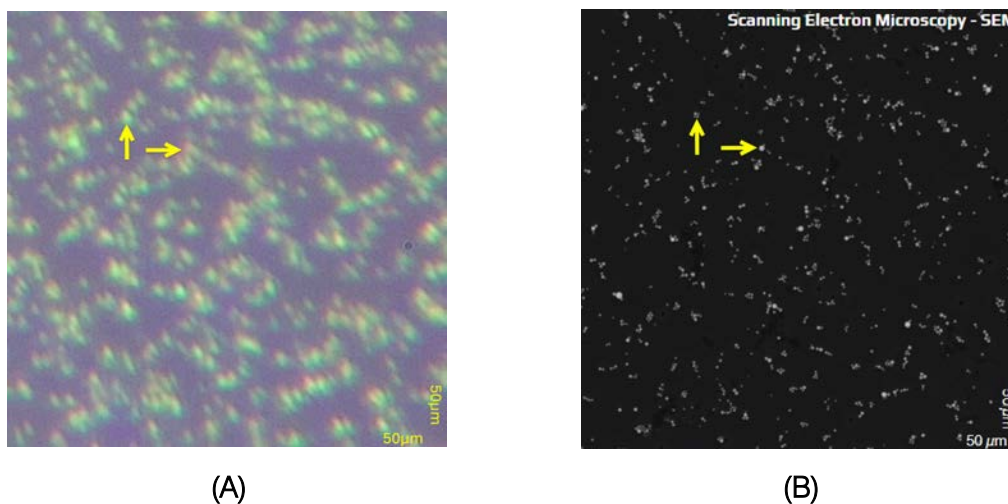


Figure 1: (A) Optical microscope image and (B) SEM image of the same region. Yellow arrows indicate identical locations, illustrating how clusters of small nanoparticles appear indistinguishable from larger particles in optical images.

Figure 2 shows a wide-field SEM image acquired in the FusionScope of a mixed sample of iron oxide and gold-coated iron oxide nanoparticles. Wide-field SEM imaging was used to rapidly survey hundreds of particles, enabling analysis of clustering behavior, spatial distribution over hundreds of microns, and particle size distributions. Both nanoparticle types were antibody-functionalized via carbodiimide crosslinking, followed by incubation with the target antigen in 0.5% BSA/PBS buffer (pH 7.4) to form antigen–antibody complexes. Particles were washed, resuspended in potassium phosphate buffer (0.01%), and 10–20 μL of solution was deposited onto TEM grids and incubated at room temperature for 1 hour prior to imaging. SEM analysis shows that antibody functionalization increased the mean radius of plain iron oxide nanoparticles from ~ 170 nm to ~ 240 nm, with corresponding size distributions shown in Figure 3 (B) and Figure 3 (C).

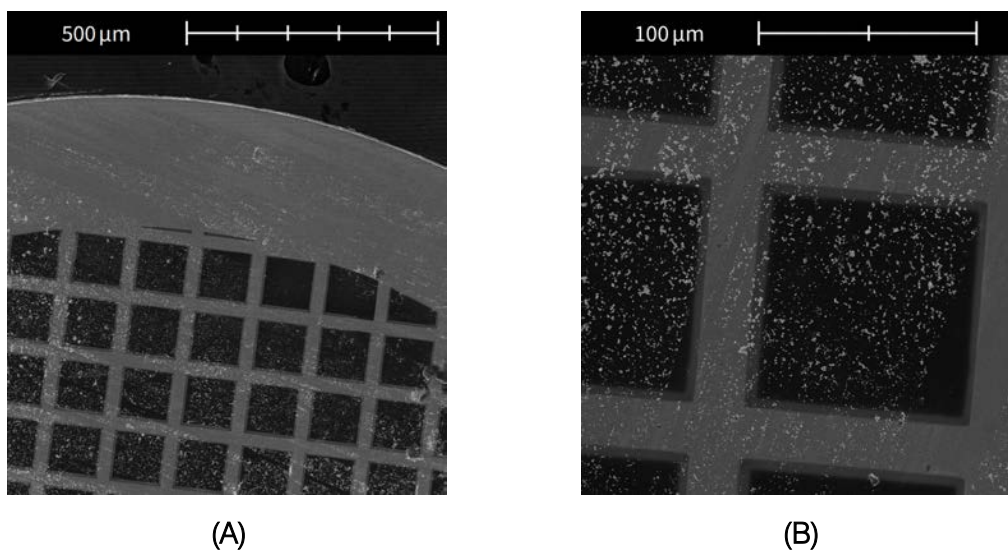


Figure 2: Wide-field SEM images of a mixture of iron oxide and gold coated iron oxide nanoparticles distributed over a TEM grid.

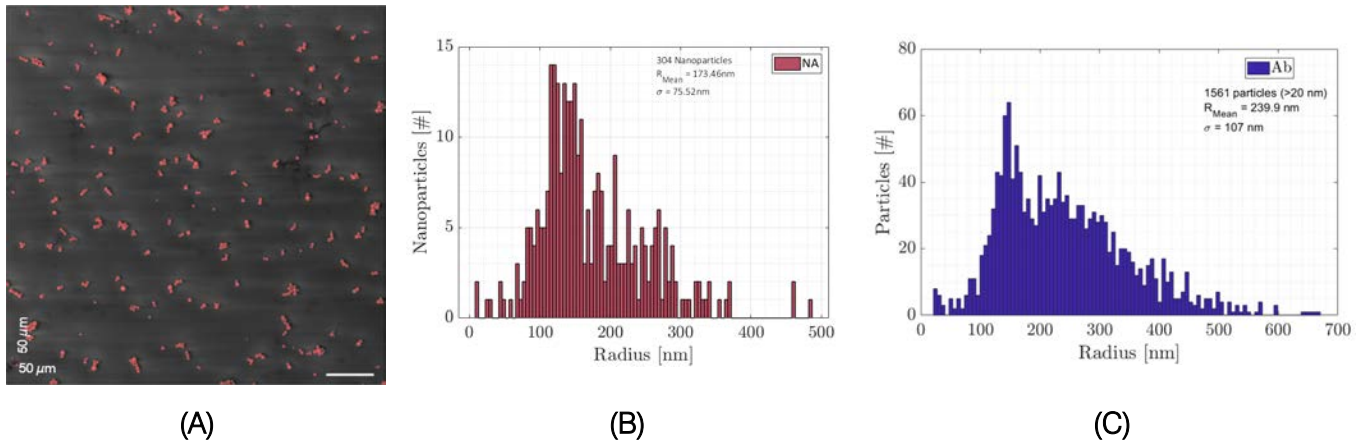


Figure 3: (A) SEM image of uncoated iron oxide nanoparticles with identified particles highlighted in red. (B) Radius distribution before antibody coating (mean ~170 nm). (C) Radius distribution after antibody coating (mean ~240 nm).

In the mixed iron oxide and gold-coated iron oxide sample, SEM imaging locates nanoparticle clusters within the wells of the TEM grid. At higher magnification, two nanoparticle species are distinguishable by gray-scale contrast (Figure 4 (A)). The tiltable sample stage and AFM allow up to 80° rotation relative to the SEM, enabling visualization of tip — sample interaction and precise positioning of the AFM tip within grid wells. Figure 4 (B) shows the AFM tip engaged with a single nanoparticle.

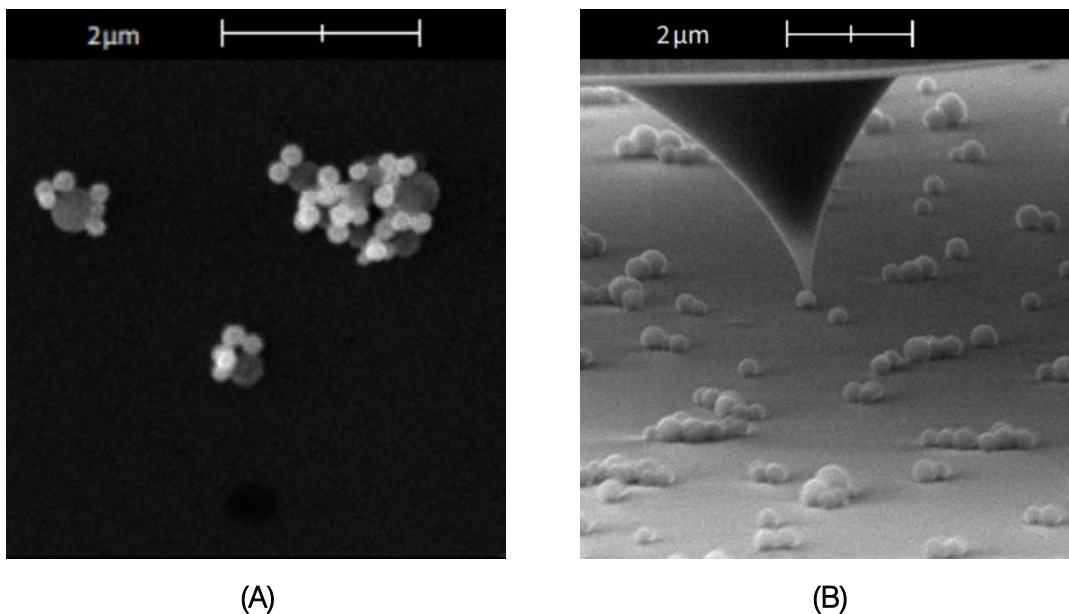
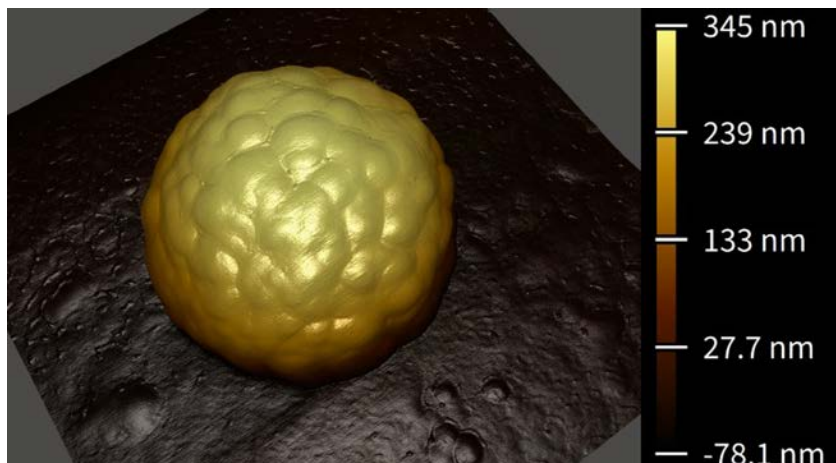


Figure 4: (A) SEM image of small clusters of nanoparticles showing both the gold coated and plain iron oxide nanoparticles. (B) SEM image of AFM tip engaged on nanoparticle.

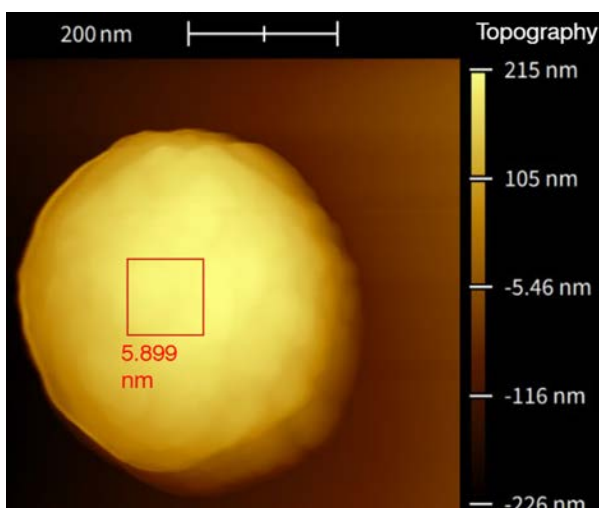
AFM with SEM

The FusionScope's integrated SEM and AFM share a common coordinate system, enabling SEM-guided positioning of the AFM tip. SEM identifies nanoparticle clusters from a wide field of view beyond the reach of optical microscopy, allowing rapid AFM scanning of individual nanoparticles with

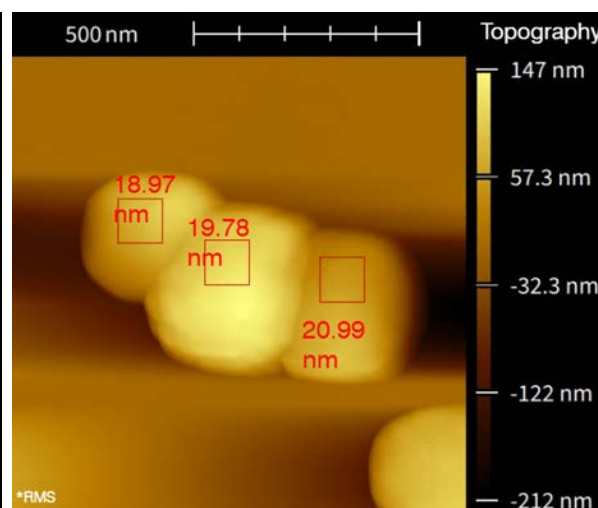
picometer-scale resolution (Figure 5 (A)). AFM topography measurements also reveal surface roughness and coating consistency: plain iron oxide nanoparticles exhibit an RMS roughness of ~ 5 nm (Figure 5 (B)), compared to ~ 20 nm for gold-coated particles (Figure 5 (C)).



(A)



(B)



(C)

Figure 5: (A) 3D AFM topography of a single plain iron oxide nanoparticle. (B) RMS roughness of plain iron oxide nanoparticles (~ 5 nm). (C) RMS roughness of gold-coated iron oxide nanoparticles (~ 20 nm).

AFM with EDS

While morphological features can suggest nanoparticle identity, EDS provides definitive elemental identification. Depositing the mixed nanoparticles onto a TEM grid minimizes background signal, enabling EDS mapping of nanoparticle clusters to distinguish gold-coated from plain iron oxide particles. Figure 6 (A) shows all detected elements, Figure 6 (B) highlights gold, and Figure 6 (C) highlights iron. The central particle exhibits a strong iron signal with no gold, identifying it as plain iron

oxide, while the surrounding smaller particles show gold with weaker iron signals, confirming them as gold-coated iron oxide.

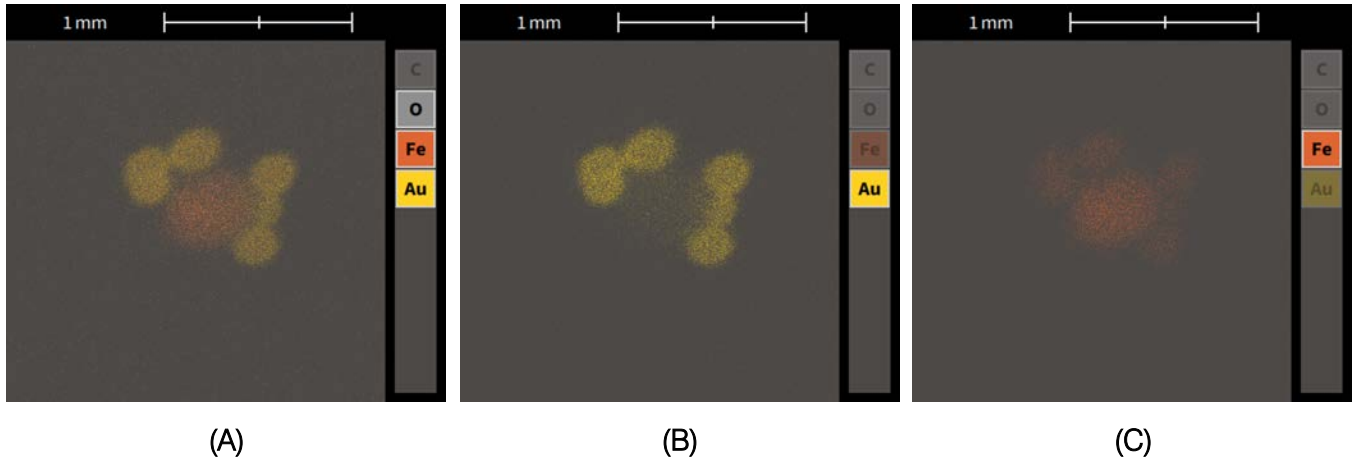


Figure 6: (A) EDS map of a nanoparticle cluster showing C, O, Fe, and Au. (B) Gold-only map indicating the central particle lacks gold. (C) Iron-only map showing a strong signal from the central particle and weaker signals from surrounding particles.

Conclusion

The FusionScope integrates SEM, AFM, and EDS into a single, correlated platform for comprehensive nanoparticle characterization. Wide-field SEM imaging identifies clusters and individual nanoparticles, AFM provides precise measurements of size, shape, and surface topography, and EDS reveals elemental composition and coatings. Because all three techniques share a common coordinate system, correlated measurements can be performed on the same nanoparticles (Figure 7), enabling confident analysis of particle size, distribution, roughness, and composition within a single system.

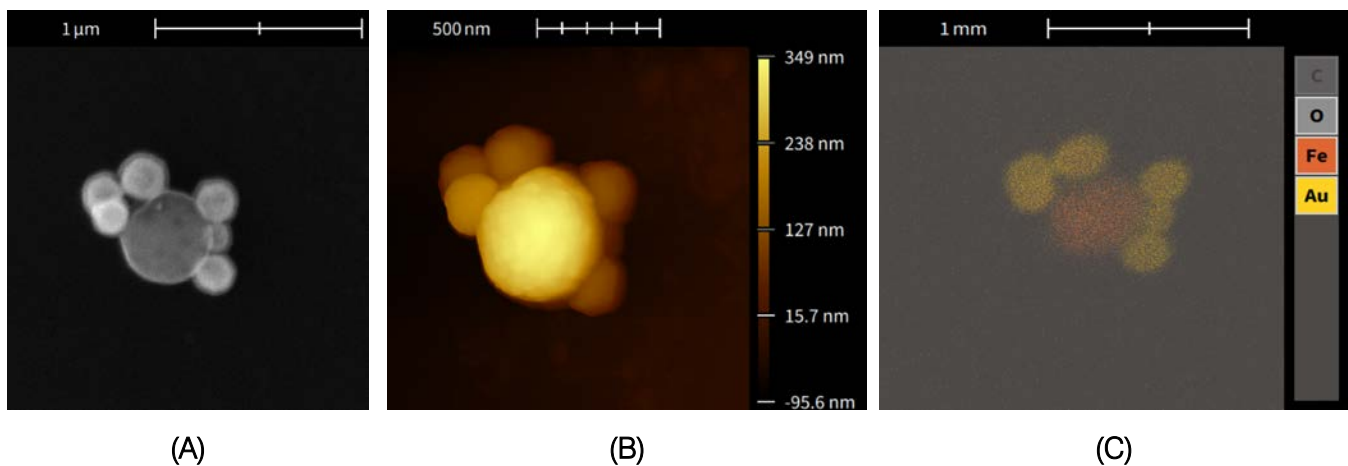


Figure 7: SEM (A), AFM (B), and EDS (C) images of the same cluster of nanoparticles taken in the FusionScope.

References

- [1] J. Sitterberg, et al. "Utilising atomic force microscopy for the characterisation of nanoscale drug delivery systems," *Eur. J. Pharm. Biopharm.*, **2010**, 74, no. 1, pp. 2-13. doi:10.1016/j.ejpb.2009.09.005.
- [2] W. Stark, et al. "Industrial applications of nanoparticles," *Chemical Society Reviews*, **2015**, 44.16, p.5793, doi: 10.1039/C4CS00362D
- [3] K.A. Altammar, "A review on nanoparticles: characteristics, synthesis, applications, and challenges." *Frontiers in Microbiology*, **2023**, 14, 1155622, doi:10.3389/fmicb.2023.1155622.
- [4] P. Kambhampati, "Nanocrystals, and Quantum Dots: What are the Implications of Size in Colloidal Nanoscale Materials?," *J. Phys. Chem. Lett.*, **2021**, 12, p. 4769. doi:10.1021/acs.jpcclett.1c00754.
- [5] J. Moger, et al., "Imaging metal oxide nanoparticles in biological structures with CARS microscopy," *Optics Express.*, **2008**, 16, pp. 3408-3419, doi:10.1364/OE.16.003408.
- [6] M. Nayak, et al., "Introduction to semiconductor nanomaterial and its optical and electronics properties," in *Metal Semiconductor Core-Shell Nanostructures for Energy and Environmental Applications, Micro and Nano Technologies*, R. K. Gupta and M. Misra, Eds., Elsevier, pp. 1-33, **2017**, pp. 1-17. doi: 10.1016/B978-0-323-44922-9.00001-6.
- [7] S. Thomas, et al., "Ceramic Nanoparticles: Fabrication Methods and Applications in Drug Delivery," *Curr. Pharm. Des.*, **2015**, 21, no. 42, pp. 6165 - 6188. doi: 10.2174/1381612821666151027153246.
- [8] M. Beach, et al., "Polymeric Nanoparticles for Drug Delivery," *Chem Rev.*, **2024**, 124, no. 9, pp. 5505–5616. doi: 10.1021/acs.chemrev.3c00705.
- [9] K. Arat, et al., "Nanoparticle Characterization with In Situ AFM-SEM-EDS," *Microscopy and Microanalysis*, **2024**, 30, doi: 10.1093/mam/ozae044.233
- [10] nanoComposix, "50 nm Ultra Uniform Gold Nanospheres," [Online]. Available: <https://nanocomposix.com/products/50-nm-ultra-uniform-gold-nanospheres?variant=41238546219097>.